View metadata, citation and similar papers at core.ac.uk
brought to you by CORE
provided by Digital.CSIC

AUSTENITE GRAIN COARSENING UNDER THE INFLUENCE OF NIOBIUM CARBONITRIDES

David San Martín, Francisca G. Caballero, Carlos Capdevila and Carlos García de Andrés*

Solid-Solid Phase Transformations Group (GITFES), Department of Physical Metallurgy, Centro Nacional de Investigaciones Metalúrgicas (CENIM), CSIC, Av. Gregorio del Amo 8, 28040, Madrid, Spain.

*Corresponding author: cgda@cenim.csic.es. Fax number: +34 91 5347425

David San Martín: dsm@cenim.csic.es

Fracisca García Caballero: fgc@cenim.csic.es

Carlos Capdevila: ccm@cenim.csic.es

Synopsis

This work investigates grain growth behaviour under the influence of pinning carbonitrides in a niobium microalloyed steel. The effect of temperature and heating rate on the grain size is studied. The grain coarsening temperature is determined as a function of the heating rate. It is found that unpinning by precipitates occurs around 40-70K below the temperature of complete dissolution of carbonitrides. Austenite grain growth is explained theoretically taking as a basis the model

proposed by *Zener*, which has been adapted for non-equilibrium kinetics, taking into account the experimental evidence that during a continuous heating, the amount of microalloyed element in solid solution is altered and different from that predicted by the solubility product.

Keywords: Grain growth, microalloyed steel, Zener model.

1. Introduction

The driving force for grain growth results from the decrease in free energy of the system. The grain boundary area is the main source of energy for grain growth process; therefore, the system will evolve to reduce its grain boundary area [1)]. Larger grains will grow at the expense of the smaller ones. Microalloying elements like vanadium, niobium and titanium have been employed in the past two decades to produce fine precipitation in the matrix. The austenite grain boundaries and dislocations are pinned by these precipitates, inhibiting their movement during the thermomechanical processing of steels [2)]. This pinning force is governed by the thermodynamic stability of second-phase precipitates in austenite [3-5)]. The temperature at which the equilibrium existing between driving forces for grain growth and pinning is broken, is defined as the grain coarsening temperature. At this temperature abnormal grain growth begins and a non-uniform grain microstructure is obtained [6)].

Austenite is the parent of the other microstructures, not only from the viewpoint that the other structures come from its decomposition, but also that it provides the framework for some of their characteristics. Shape and size of the austenite grain will determine the rates of transformation through points of nucleation and paths for transformation. The understanding of the grain coarsening behaviour is essential for predicting final mechanical properties of steels. In this sense a uniform fine-grained microstructure is very important. Therefore, due to its importance, the experimental determination and

accurate theoretical prediction of the prior austenite grain size (*PAGS*) under the influence of pinning precipitates and the determination of the grain coarsening temperature becomes of the greatest importance in metallurgical studies [7-12].

Zener [13] was the first to obtain a quantitative theoretical expression to evaluate the influence of precipitate inhibiting effect on grain boundary motion. This model balances the force for grain growth that arises from the decrease in grain boundary area per unit volume, against the pinning force caused by precipitates present in the matrix. From this relation the following general equation is obtained,

$$\overline{D}_{crit} = \beta \frac{r}{f} \qquad (1)$$

Where $\overline{D}_{crit}$ is the average critical 3-D prior austenite grain size (*3DPAGS*) of the microstructure in the presence of a volume fraction of precipitates, *f*, that have a mean radius, *r*. The value of β depends on factors such as the geometry of precipitates and austenite grains, or coherency between precipitate and matrix. This factor is usually considered as constant for a given steel. Other authors [14-22] have given several expressions since the seminal work by Zener, most of which incorporate Zener's ideas in some way. According to these expressions, depending on the size and the amount of the dispersed precipitates, the grain growth rate and the *3DPAGS* will be greatly

affected. Table 1 shows some values of factor β that can be found in the literature.

The present article describes the austenite grain growth during a continuous heating at different rates in a niobium microalloyed steel. A set of expressions is proposed to describe the austenite growth kinetics under the influence of pinning precipitates during a continuous heating at a constant rate.

2. Materials and experimental procedure

A low-carbon niobium microalloyed steel has been studied. Its chemical composition is listed in Table 2.

Cylindrical samples of 3 mm in diameter and 12 mm in length were used to reveal grain boundaries by the thermal etching method [24, 25]. For this purpose, a surface 2 mm in width was generated along the longitudinal axis of samples by polishing and finishing with 1μm diamond paste. Later on, these samples were austenitized in vacuum (>1Pa) at different heating rates (HR) and at temperatures ranging from 1183K to 1523K (Tγ). Subsequently samples were cool down to room temperature at 1K/s. In Table 3, heating rates and austenization temperatures studied are shown. These samples do not require metallographic preparation after heat treatment, and the prior austenite grain boundaries are revealed without chemical etching.

The average austenite grain size was measured using an image analyser. Pictures of the prior austenite microstructure were acquired

and processed in order to generate a binary image in which prior austenite grain boundaries were shown in black. From this binary images the average area of austenite grains in 2-D, $\overline{A}$, was obtained.

In this work it will be considered that the three dimensional prior austenite grains can be represented as tetrakaidecahedrons. This polyhedron satisfies the space-filling and surface tension requirements. Hull and Houk [23] used a wire frame model of this polyhedron to get the distribution of areas of intersection with a given reference plane. They found that the mean, $\overline{A}$, and maximum, A_{max}, areas intersected could be related through the equation $\overline{A}/A_{max} = 0.546$. Taking into account that the distance between square faces of a tetrakaidecahedron can be written as $\overline{D} = 1.069\sqrt{A_{max}}$, a value for the average 3-D prior austenite grain size (*3DPAGS*) can be given,

$$\overline{D} = 1.447\sqrt{\overline{A}}\,. \qquad (2)$$

A two-step extraction carbon replica method has been used to examine and identify precipitates present in the austenite grain boundaries [26-29]. In a first stage, triacetylcellulose thin films, which can be easily pasted onto the specimen surface with methyl acetate and then stripped off, are obtained. The second step consists in evaporation of carbon onto the plastic film in a high vacuum chamber. Carbon replicas obtained using this method where examine using a Jeol Jem 2010 TEM, at an

operating voltage of 200 kv, with an energy dispersive spectroscopic (EDS) analyser Oxford Inca.

3. Results and Discussion

3.1. Experimental results

Figure 1 shows the evolution of the *3DPAGS* during a continuous heating at 0.05, 0.5 and 5K/s. Figure 2 shows the prior austenite microstructure formed after heating the sample to three different temperatures at a rate of 5K/s.

It is well known that the *3DPAGS* in plain carbon steels increases exponentially with temperature [4)]. However, in microalloyed steels is usual to observe two-step grain growth [4, 6, 30, 31)]. In the niobium microalloyed steel studied in the present work this two-step growth is found. The sluggish grain growth in the lower range of temperatures is associated with the existence of precipitates that pin the boundaries, inhibiting their movement. As temperature is raised, several precipitates dissolve while others coarsen. Thus, some grain boundaries are free to move and the average *3DPAGS* of the microstructure will grow. As it is shown in Figure 1, grain growth is very sensitive to heating rate. The faster the heating rate is, the slower the *3DPAGS* coarsens.

Carbon replicas showed that niobium carbonitrides were precipitated in the matrix (Figure 3). ‘Cu’ peaks in the EDS spectrum corresponds to the copper mesh that supports the replica. The average radius for

carbonitrides measured from carbon replicas just above Ac_3 temperature was r_0=0.01±0.004 μm. Ac_3 is the temperature at which the process of austenitization is completed and it was experimentally determined for this steel at 1168±3K [32].

3.2. Grain coarsening temperature (T_{GC})

The grain coarsening temperature (T_{GC}) is usually defined as the temperature at which abnormal grain growth begins and grain size grows up very rapidly [6, 33]. As it was mentioned above (Figure 1), in the studied steel a two-step grain growth is observed. During heating the initial distribution of austenite grains evolves homogeneously under the influence of pinning niobium carbonitrides until the T_{GC} is reached. At this point, some grains grow fast while others remain pinned, leading to a duplex austenite grain size microstructure. Further heating results in the unpinning of all grain boundaries and homogeneous growth is reached again. Figure 1 shows that the temperature T_{GC} lays around 1373K for the three heating rates. In order to be more precise in the determination of T_{GC}, experimental points corresponding clearly to the first step in Figure 1 (1183, 1223, 1273 and 1323K), and those related with the second step of growth (1423, 1473 and 1523K) have been approximated by an exponential function of temperature of the form $k\exp(-q/T)$. As a first approach it has been considered that the T_{GC} is that at which the exponential functions corresponding to each step intersect. In Figure 4 the points of intersection between exponential functions corresponding to each

step and heating rate are shown in detail. Results obtained are shown in Table 4.

From this table several conclusions can be drawn. First, T_{GC} lays around 40-70K below the temperature of complete dissolution of carbonitrides (T_{DISS}), later calculated for this steel. Grain boundary unpinning requires that the precipitates dissolve and grow only to an extent at which the pinning force falls below a critical value and this happens well below T_{DISS}. This result is in agreement with the experimental work of Palmiere et al. [33], Cuddy and Raley [6] and Gladman and Pickering [3]. Second, the faster the heating rate, the higher the grain coarsening temperature. This is due to the fact that with high heating rates, equilibrium conditions are not attained. Non-equilibrium leads to a decrease in the rate of dissolution and coarsening of precipitates. Finally, the faster the heating rate, the lower the *3DPAGS* at which grain coarsening starts.

Fig 5 represents T_{GC} measured by Palmiere et al. [33] and Cuddy and Raley [6] against niobium content of the steel. Data corresponding to steels from these authors have similar amount of carbon equivalent $C_{eq}=C+(12/14)N$=0.07-0.09% and were obtained after heating for 30 minutes at the corresponding austenitizing temperature. *C* and *N* in this formula represent the carbon and nitrogen content in wt-%, respectively. From this figure, it seems to be a tendency to have a higher T_{GC} the higher the *Nb* content in the steel, as long as sufficient C_{eq} content is available to form more carbonitrides. The black circle

refers to the steel of the present work for a heating of 0.05K/s and it could be seen that this result perfectly fits in the curve.

3.3. Evolution of the radius and volume fraction of carbonitrides

During heating, dissolution of niobium carbonitrides takes place. This process has two effects; a direct effect in reducing the volume fraction of precipitates and an indirect effect of increasing their rate of ripening (increasing the size of precipitates) by providing a higher solute level in solid solution. According to equation (1), both effects contribute to the increase of the critical grain size $\overline{D}_{crit}$ during reheating. According to Lifshitz and Slyozov [34] the variation of the radius of niobium carbonitride during an isothermal treatment at a temperature T can be stated as,

$$r^3 = \left(r_0^3\right) + \left(4\sigma V_m D_V \left[Nb\right] t\right) / \left(9RT\right) \qquad (3)$$

Where r is the radius of carbonitrides in microns, r_0 is the radius of precipitates at the end of austenite formation, T is the absolute temperature, t is time in seconds, σ is the interfacial energy between precipitate and matrix, V_m is the molar volume of carbonitrides, D_V is the volume diffusion of niobium in austenite, [Nb] is the amount of niobium, in wt-%, in solid solution in equilibrium with the austenite matrix and R is the universal gas constant. The diffusivity of niobium is much lower than the diffusivity of carbon or nitrogen in austenite;

hence, niobium volume diffusion is supposed to be the rate controlling process during ripening of carbonitrides. The amount of niobium in solid solution can be obtained from the solubility product of niobium carbonitrides, which is given by following equation [33],

$$Log[Nb][C+(12/14)N]=2.26-(6770/T) \quad (4)$$

Where C and N are carbon and nitrogen, in wt-%, in solid solution respectively, and T is temperature in K. Taking into account that the microstructure evolves during a continuous heating at a constant rate, equation (3) has been differentiated in time and the relation $\theta = dT/dt$, where θ is the heating rate, has been introduced. Finally, integrating the resultant equation in [r_0, r] and [Ac_3 ,T] intervals on the left and right sides, respectively,

$$r^3 = r_0^3 + (4\sigma V_m/9R\theta)\int_{A_{c3}}^{T}(D_V[Nb]/T)dT \quad (5)$$

Introducing composition in equation (4), a T_{DISS} of 1437K is obtained, very similar to that predicted by MTDATA software [35] (1423K), assuming that in the initial microstructure all Nb was present in the form of carbonitrides. In Figure 6 the equilibrium volume fraction of carbonitrides, f, obtained with MTDATA, and the evolution of the radius with temperature and heating rate (equation (5)) have been

represented. The values used for different physical parameters, for the calculation of equation (5), are listed in Table 5.

3.4 Theory of grain growth under the influence of pinning carbonitrides during a continuous heating

In this work, a new model to describe the austenite grain coarsening under the influence of niobium carbonitrides during a continuous heating is proposed. In this sense, it will be assumed that the equilibrium volume fraction of carbonitrides, *f*, obtained with MTDATA and the equilibrium content of niobium in solid solution, [*Nb*], is reached at each austenitization temperature only for a heating rate of 0.05K/s. In order to quantify the average *3DPAGS* under the influence of pinning carbonitrides, the following expression is considered,

$$\overline{D}_{crit} = \beta\left(\alpha\frac{r}{f}\right) \qquad (6)$$

In this equation, the parameter α gives an estimation of the effect of the non-equilibrium continuous heating on the value of r/f. Under equilibrium conditions (0.05K/s), α=1. The equation (6) is only valid for temperatures before the grain coarsening temperature (T_{GC}). Therefore, according to results in Table 4, for a heating rate of 0.05K/s this equation is only valid for experimental values raging

from 1183K to 1323K, while for 0.5 and 5K/s is valid from 1183K to 1373K. Figure 7 shows the evolution of the experimental average critical *3DPAGS*, $\overline{D}_{crit}$, against the calculated value of r/f for each heating temperature and in the range of temperatures mentioned before. From the slope of the linear fits (dashed lines) of the points corresponding to each heating rate, parameters β and α can be deduced. Bearing in mind that β is constant with temperature and heating rate (for a given steel), and taking into account the approximation that at 0.05K/s equilibrium is attained at each temperature (and thus $\alpha_{0.05}$=1), Table 6 lists the values of β and α obtained from Figure 7. As it would be expected, parameter α decreases as the heating rate increases. In this figure, the experimental values have been compared with limits given by Gladman theory [38] (thick lines). The value of β obtained is also similar to estimations predicted or measured by other authors (see Table 1).

Equation (5) and (6) along with values in Table 6 and calculations of the volume fraction of carbonitrides made with MTDATA allow predicting the evolution of the *3DPAGS* in a niobium microalloyed steel for temperatures below T_{GC} during a continuous heating. In Figure 8 measured values of the average *3DPAGS* (open points) are compared with those obtained using equation (6) (dot lines) in the range of temperatures below T_{GC} (given in Table 4). Experimental and theoretical values are in good agreement.

Finally, from results shown above, the evolution of the pinning driving force of niobium carbonitrides with temperature for the

heating rates studied can be calculated. The pinning driving force associated with niobium carbonitrides can be written as,

$$G_Z = k_1 \gamma \frac{f}{r} \tag{7}$$

Where γ is the grain boundary energy and k_1 is a parameter dependent on the geometry of carbonitrides and coherency between precipitates and the matrix. On the other hand, the driving force for grain boundary migration is inversely proportional to the average *3DPAGS* ($\overline{D}$),

$$G_{GG} = k_2 \frac{\gamma}{\overline{D}} \tag{8}$$

Where k_2 depends on the geometry of three dimensional austenite grains. When grain boundaries are pinned ($T<T_{GC}$), $G_Z=G_{GG}$ and $\overline{D}$ corresponds to $\overline{D}_{crit}$ in equation (6). Thus, the following expression is achieved,

$$k_1 = k_2 / \alpha\beta \tag{9}$$

Therefore, the pinning force (equation (6)) can be rewritten as,

$$G_Z = \frac{k_2 \gamma}{\alpha \beta} \frac{f}{r} = \frac{\eta}{\alpha} \frac{f}{r} \qquad (10)$$

Where $\eta = k_2 \gamma / \beta$. Assuming the geometry of prior austenite grains as tetrakaidecahedrons (k_2=3.35 [39]) and taking γ=0.8x10^{-12}J/μm^2 [40], it is found that η=3.8x10^{-12}J/μm^2. Figure 9 shows the evolution of the real pinning force, G_Z, given by equation (10), with temperature for each heating rate. An increase in the heating rate affects the dissolution and coarsening kinetics of carbonitrides, delaying these processes and causing the grain boundary pinning to increase. Therefore, the higher the heating rate, the larger and finer distribution of carbonitrides is present in the microstructure.

4. Conclusions

1. The niobium microalloyed steel studied shows a two-stage grain growth during a continuous heating due to the existence of niobium carbonitrides precipitates in the matrix. The grain coarsening temperature (T_{GC}) has been obtained. It has been found that as the heating rate increases, T_{GC} temperature increases and the grain size at that temperature decreases. T_{GC} temperature lays around 40-70K below the temperature of complete dissolution of carbonitrides (T_{DISS}).

2. Based on the theory by *Zener*, a new model has been proposed to describe the austenite grain coarsening under the influence of niobium

carbonitrides during a continuous heating at a constant rate. It has been found a good correlation between the model proposed and experimental data.

3. An expression has been obtained to describe the pinning force exerted by a distribution of niobium carbonitrides during a continuous heating at different rates.

5. Acknowledgement

The authors acknowledge financial support from Spanish Ministerio de Ciencia y Tecnología (Project PETRI 1995-0667-OP). F.G. Caballero would like to thank Spanish Ministerio de Ciencia y Tecnología for the financial support in the form of a Ramón y Cajal contract (Programa RyC 2002).

6. References

1) H.V. Atkinson: Acta Metall. **36** (1988) 469-491.

2) N.T. Baker: *Future Developments of Metals and Ceramics*, edited by J.A. Charles, G.W. Greenwood and G.C. Smith (Institute of Materials, London, 1992), pp. 75.

3) T. Gladman and F. B. Pickering: J. Iron Steel Inst. **205** (1967) 653-664.

4) R. Coladas, J. Masounave, G. Guérin and J.-P.Bailón: Met. Sci. **November** (1977) 509-516.

5) G.R. Speich, L. J. Cuddy, C.R. Gordon, and A.J. DeArdo: *Phase Transformations in Ferrous Alloys*, A. R. Marder and J. I. Goldstein eds (TMS-AIME, Warrendale, PA, 1984) pp. 341.

6) L.J. Cuddy and J. C. Raley: Metall. Trans. A **14** (1983) 1989-1995.

7) H. Ohtani, F. Terasaki,T. Kunitake: Trans. Iron Steel Inst.Jpn. **12** (1972) 118-127.

8) N. J. Petch: J. Iron Steel Inst. **174** (1953) 25-28.

9) A. Grange: Trans. Am. Soc. Met. **59** (1966) 26.

10) S. Kim, S. Lee and B. S. Lee: Mater. Sci. Eng. A **359** (2003) 198-209.

11) J. Kusiak and R. Kuziak: J. Mater. Process. Tech. **127** (2002) 115-121.

12) A. Di Schino, M. Barteri and J.M. Kenny: J. Mater. Sci. **38** (2003) 4725-.

13) C. Zener, quoted by C. S. Smith: Trans. AIME **175** (1948) 15-51.

14) M. Hillert: Acta Metall **13** (1965) 227-238.

15) T. Gladman: Proceedings of the Royal Society **294A** (1966) 298.

16) N. A. Haroun and D. W. Budworth: J. Mater. Sci **3** (1968) 326-328.

17) N. A. Haroun: J. Mater. Sci **15** (1980) 2816.

18) P. Hellman and M. Hillert: Scand. J. Metall. **4** (1975) 211-219.

19) N. Ryum, O. Hunderi and E. Nes: Scr. Metall **17** (1983) 1281

20) E. Nes, N. Ryum and O. Hunderi: Acta Metall **33** (1985) 11.

21) P.R. Rios: Acta Metall. **35** (1987) 2805-2814.

22) Y. Ogino: Tetsu-to-Hagane **57** (1971) 533.

23) F. C. Hull and W. J. Houk: J. Met. **April** (1953) 565-572

24) C. García de Andrés, M. J. Bartolomé, C. Capdevila, D. San Martín, F. G. Caballero, V. López: Mater. Charact. **46** (2001) 389-398.

25) C. García de Andrés, F.G. Caballero, C. Capdevila, D. San Martín: Mater. Charact. **4** (2003) 121-127.

26) G. R. Booker, J. Norbury: British J. Appl. Phys. **8** (1957) 109

27) C. P. Scott, D. Chaleix, P. Barges, V. Rebischung: Scr. Mater. **47** (2002) 845-849.

28) S. G. Hong, H. J. Jun, K. B. Kang, C. G. Park: Scr. Mater. **48** (2003) 1201-1206.

29) A. Fukami: Jeol News, **July** (1967) 5-7.

30) F. Peñalba, C. García de Andrés, M. Carsí, F. Zapirain: J. of Mater. Sci. **31** (1996) 3847-3852.

31) C. García de Andrés, C. Capdevila, F. G. Caballero, D. San Martín: J. Mater. Sci. **36** (2001) 565-571.

32) D. San Martín: *Modelización de la cinética de austenización y crecimiento de grano austenítico en aceros ferrítico-perlíticos*, PhD Thesis, (Universidad Complutense of Madrid, Spain, 2003) pp.159.

33) E.J. Palmiere, C.I. Garcia and A.J. DeArdo: Metall. Mater. Trans. A **25** (1994) 277-286.

34) I.M. Lifshitz and V.V. Slyozov: J. Phys. Chem. Solids **19** (1961) 35-50.

35) H. Davies: *MTDATA* (National Physical Laboratory, Teddington, UK, 2003).

36) H. S. Zurob, C.R. Hutchinson, Y. Brechet and G. Purdy: Acta Mater. **50** (2002) 3075-3092.

37) B. Dutta, E. Valdés, C.M. Sellars: Acta Metall. Mater. **40** (1992) 653.

38) T. Gladman: *The Physical Metallurgy of Microalloyed Steels* (The Institute of Materials, London, UK, 1997) pp.176.

39) J.W. Cahn: Acta Metall., **4** (1956) 449-459.

40) P. A. Manohar, D.P. Dunne, T. Chandra and C.R. Killmore: ISIJ Int. **36** (1996) 194-200.

Number of letters and words

Letters: 18902

Words: 3598

List of captions of Tables.

Table 1 Value of β (equation (1)) found in the literature.

Table 2 Chemical composition (mass%)

Table 3 Heating rates and austenitization temperatures

Table 4 Grain coarsening temperatures and corresponding *3DPAGS*.

Table 5 Parameters used for the calculation of equation (3).

Table 6 Experimental β, α parameters

List of captions of Figures.

Figure 1 Evolution of the 3-D prior austenite grain size (*3DPAGS*) for three different heating rates.

Figure 2 Prior austenite microstructure obtained after heating at 5K/s; a) 1323K, b) 1423K and c) 1523K.

Figure 3 Niobium carbonitride precipitated in the matrix

Figure 4 Determination of the grain coarsening temperature

Figure 5 Evolution of the grain coarsening temperature, T_{GC}, with niobium content of the steel (experimental data from the work of *Palmiere et al* [33] and *Cuddy et al* [6]).

Figure 6 Evolution of the equilibrium volume fraction of niobium carbonitrides and the radius as a function of the heating rate and temperature

Figure 7 Relationship between average critical *3DPAGS*, $\overline{D}_{crit}$, and r/f for the three heating rates (open circles, squares and triangles) compared with limits given by *Gladman* [3] (thick lines).

Figure 8 Evolution of the experimental (open points) and theoretical (dot lines) values of $\overline{D}_{crit}$ during a continuous heating.

Figure 9 Evolution of the pinning driving force due to niobium carbonitrides during a continuous heating as a function of the heating rate and temperature.

Tables

Table 1 Value of β (equation (1)) found in the literature.

Zener [13]	Hannerz [14]	Gladman [15]	Hellman-Hillert [16]	Rios [17]	Ogino [18]
3.41	0.44	$(2.56)\,\pi\left[(1/4)-(1/3Z)\right]^{**}$	$(1.71)/\xi^{*}$	0.43	0.33

*Normally $1.3<\xi<1.6$. **Z is the ratio of diameter of growing grains to matrix grains ($\sqrt{2}$ <Z<2). Since all the authors consider two-dimensional grain radius instead of three-dimensional diameter in their calculation, in this table, their values have been multiplied by a factor of '2.56' following the work of Hull and Houk [23], $D_{crit}(3D)=2.56R_{crit}(2D)$.

Table 2 Chemical composition (mass%)

C	Mn	Si	S	P	Nb	Cu	Cr	Ni	Mo	Al	N
0.11	1.47	0.27	0.013	0.015	0.031	0.011	0.03	0.03	0.006	0.039	0.0051

Table 3 Heating rates and austenitization temperatures

Heating rate, HR/Ks^{-1}	Austenitization temperature, $T\gamma$/K
0.05, 0.5, 5	1183, 1223, 1273, 1323, 1373, 1423, 1473, 1523

Table 4 Grain coarsening temperatures (T_{GC}) and corresponding 3-D prior austenite grain size (*3DPAGS*).

Heating rate, HR/Ks^{-1}	Grain coarsening temperature, T_{GC}/K	3-D prior austenite grain size, *3DPAGS*/μm
0.05	1363	32
0.5	1385	22
5	1393	15

Table 5 Parameters used for the calculation of equation (3).

Parameter	Symbol	Value	Reference
Bulk diffusion of *Nb*	D_0/μm^{2}s^{-1}	0.83x10^8	36
Bulk diffusion of *Nb*	Q/kJmol^{-1}	266.5	36
Interfacial energy	σ/Jμm^{-2}	0.5x10^{-12}	37
Molar volume *NbCN*	V_m/μm^{3}mol^{-1}	1.28x10^{13}	37
Universal gas constant	R/JK^{-1}mol^{-1}	8.31	
Initial radius *NbCN*	r_0/μm	0.01±0.004	

Table 6 Experimental β, α parameters

Heating rate, HR/Ks^{-1}	α	β
0.05	1	0.44
0.5	0.86	0.44
5	0.80	0.44

Figures

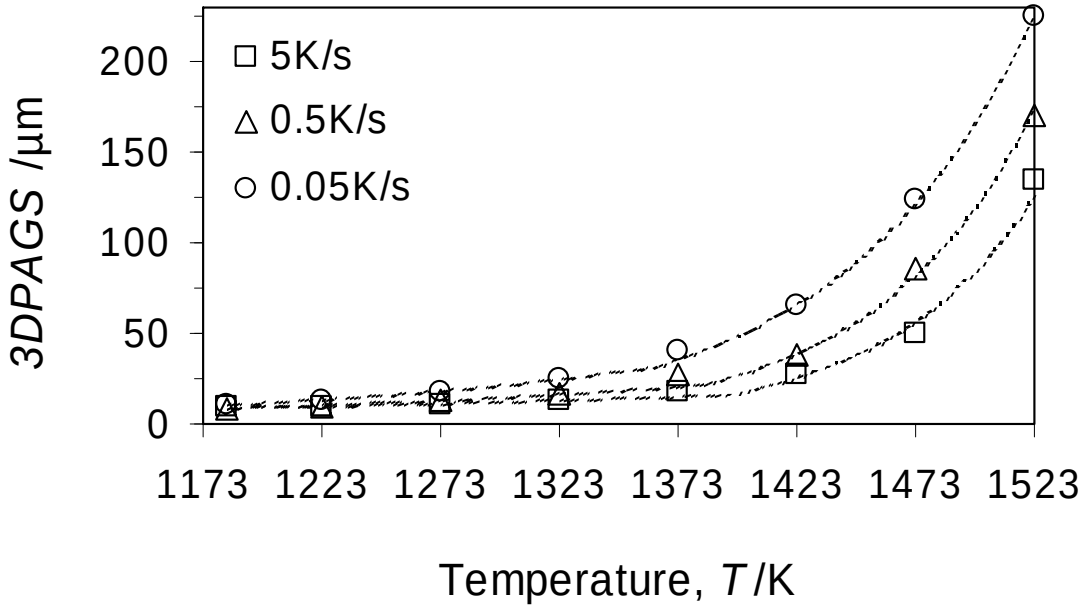

Figure1 Evolution of the 3-D prior austenite grain size (*3DPAGS*) for three different heating rates.

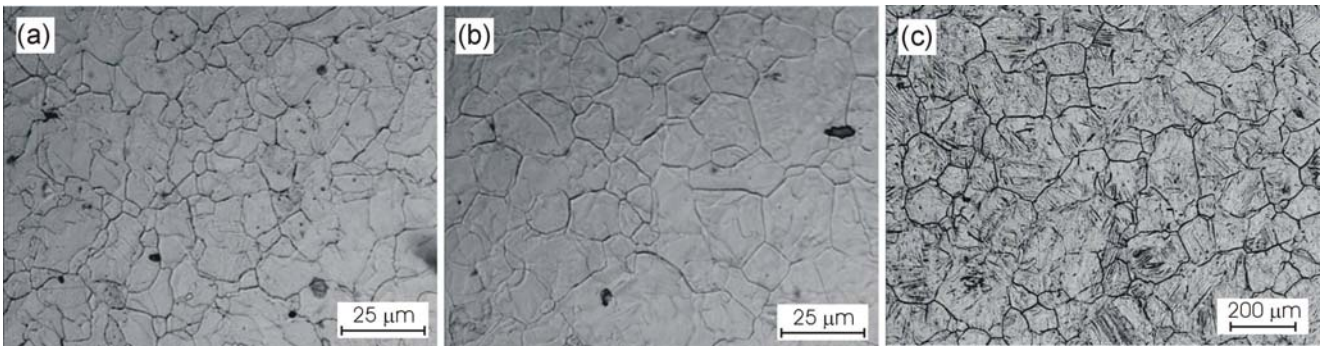

Figure 2 Prior austenite microstructure obtained after heating at 5K/s;

(a) 1323K, (b) 1423K and (c) 1523K.

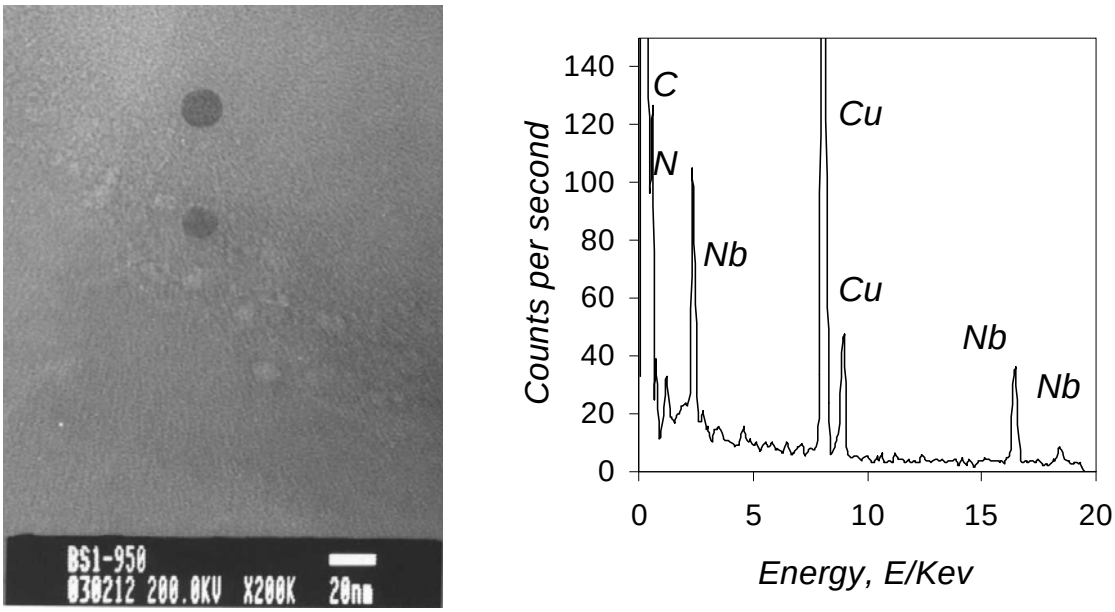

Figure 3 Niobium carbonitride precipitated in the matrix.

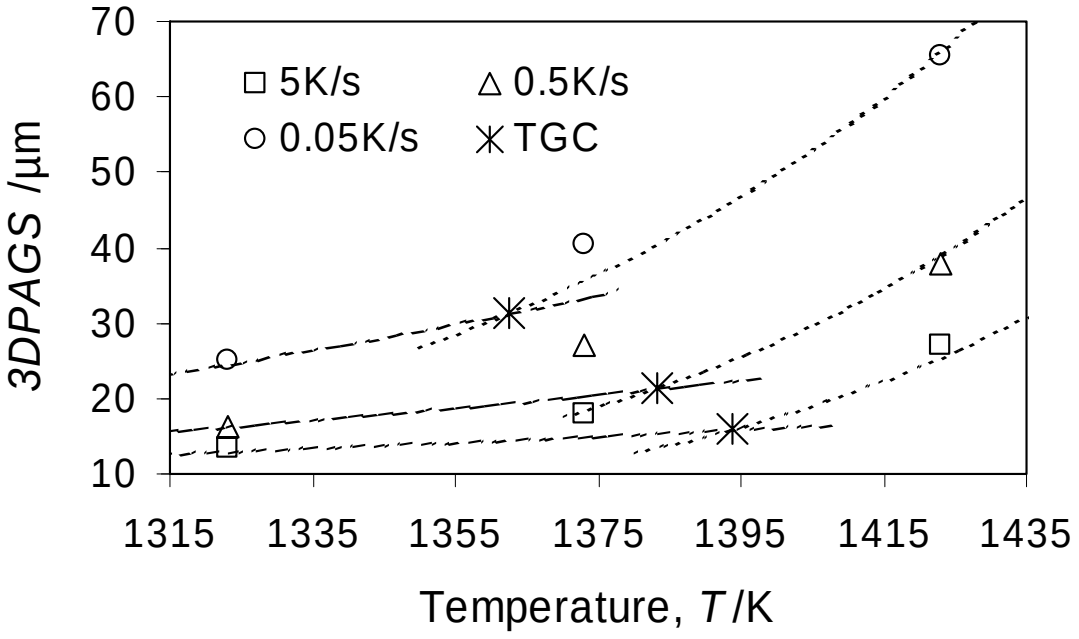

Figure 4 Determination of the grain coarsening temperature

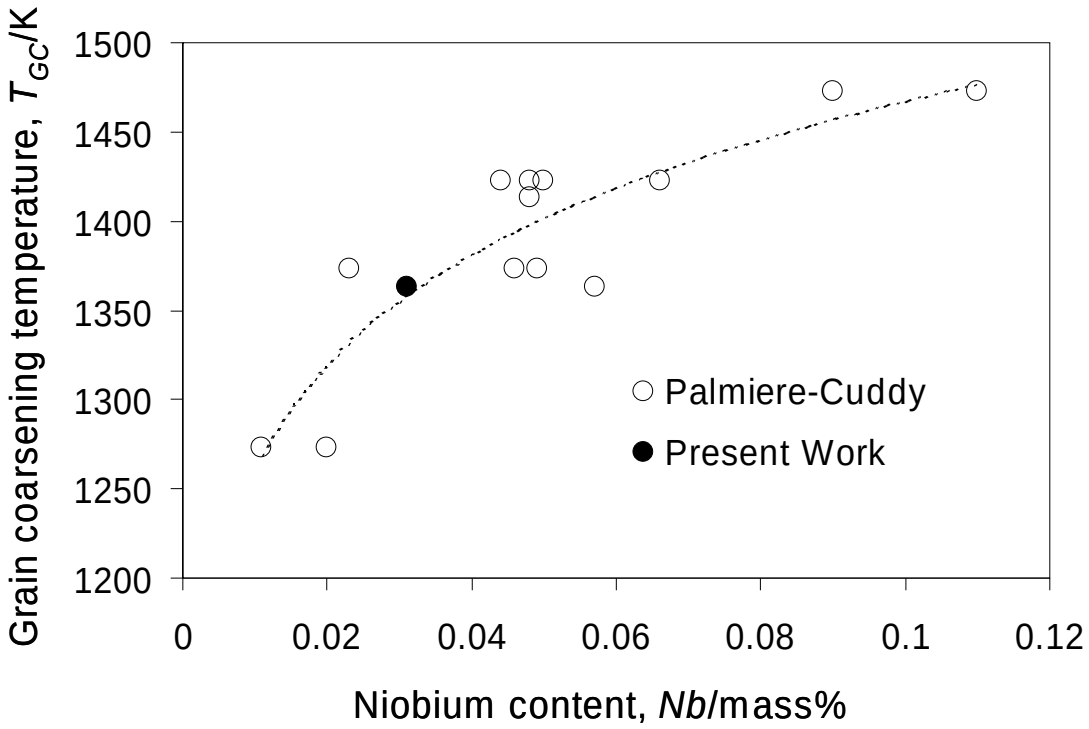

Figure 5 Evolution of the grain coarsening temperature, T_{GC}, with niobium content of the steel (experimental data from the work of Palmiere et al [33] and Cuddy and Raley [6]).

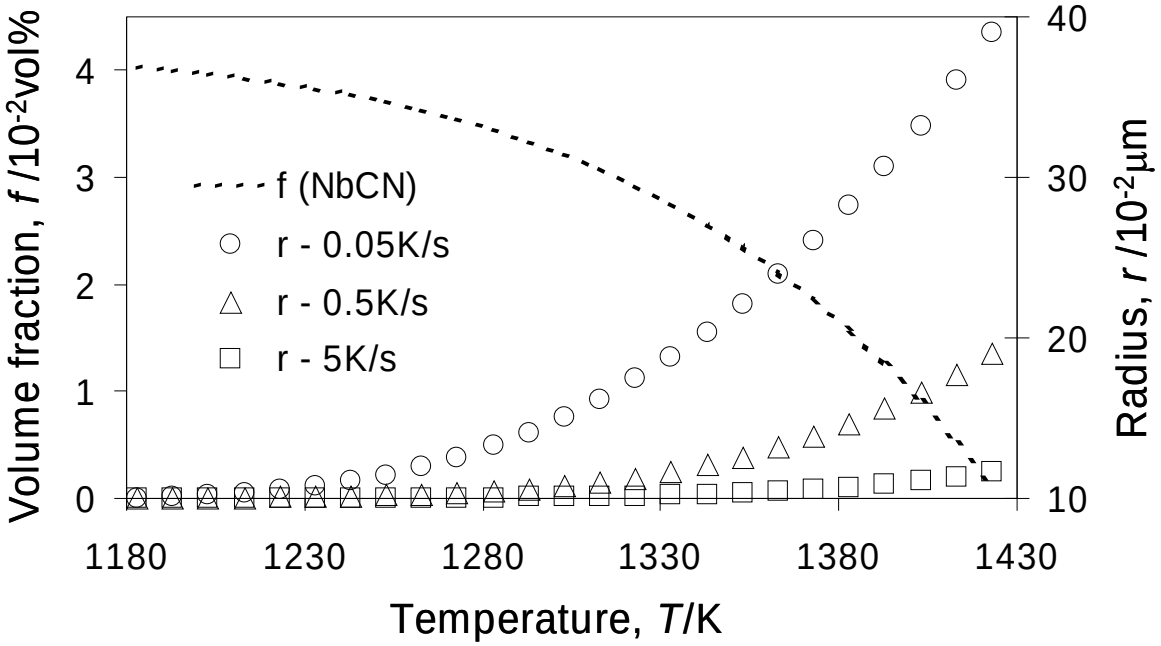

Figure 6 Evolution of the equilibrium volume fraction and the radius of niobium carbonitrides as a function of the heating rate and temperature.

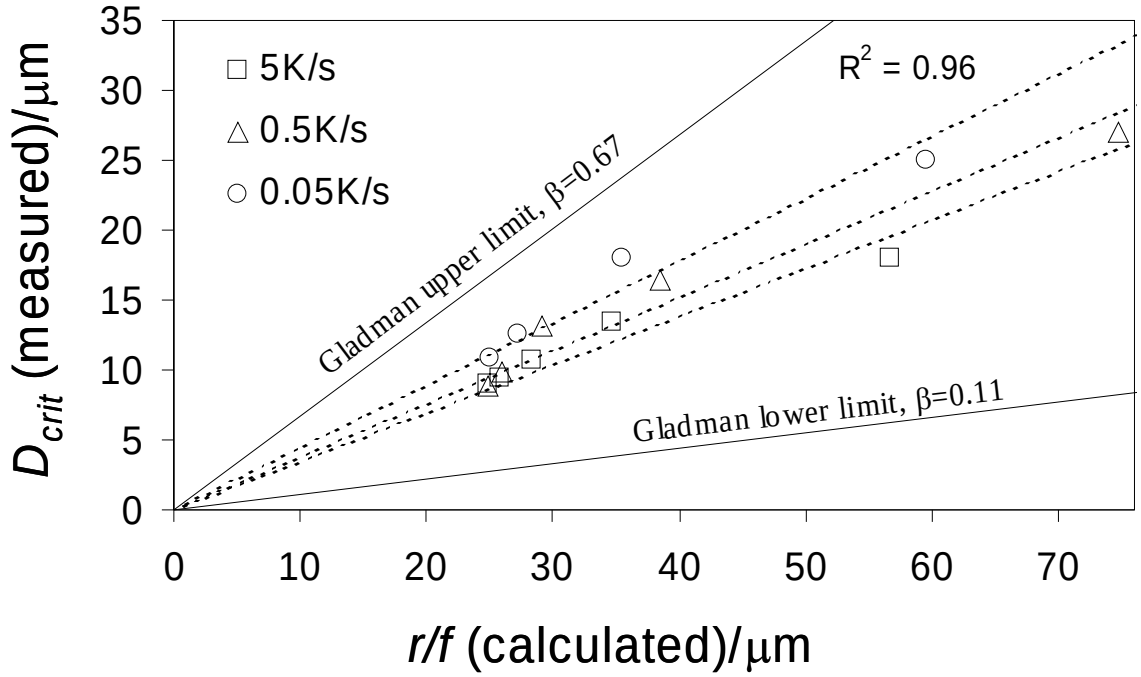

Figure 7 Relationship between average critical *3DPAGS*, $\overline{D}_{crit}$, and r/f for the three heating rates (open circles, squares and triangles) compared with limits given by *Gladman* [3] (thick lines).

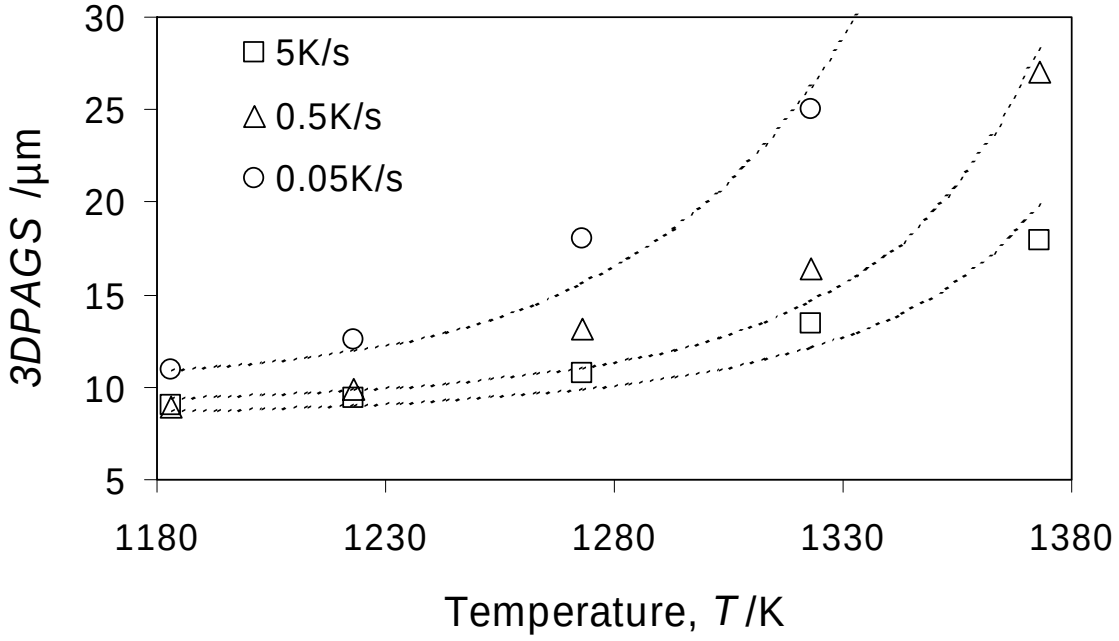

Figure 8 Evolution of the experimental (open points) and theoretical (dot lines) values of $\overline{D}_{crit}$ during a continuous heating.

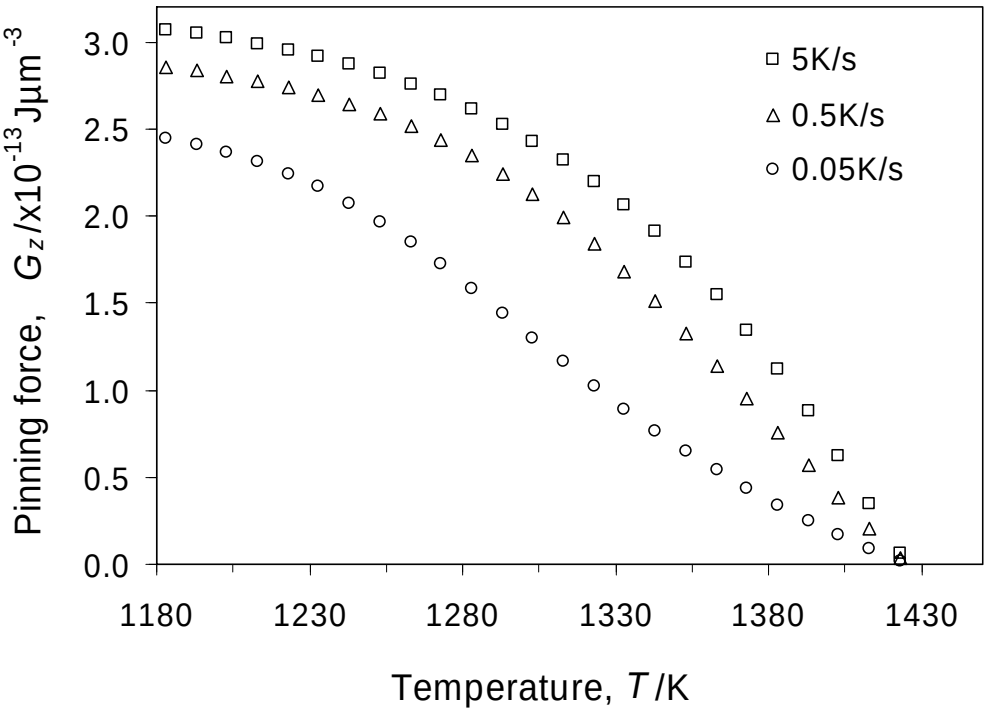

Figure 9 Evolution of the pinning driving force due to niobium carbonitrides during a continuous heating as a function of the heating rate and temperature.